Reconfigurable Wireless Power Transfer Systems With High Energy Efficiency Over Wide Load Range

Wenxing Zhong, *Member, IEEE*, and S. Y. (Ron) Hui, *Fellow, IEEE*

***Abstract*—Optimum energy efficiency in a wireless power transfer (WPT) system usually occurs only at a specific load value while the load such as a battery is normally not constant. A major challenge in WPT is, therefore, to achieve high energy efficiency over a wide load range. Previously, impedance transformation methods such as dc–dc converters and use of a relay coil have been used to transform the practical load resistance to the optimum (or near-optimum) value. In this paper, a new approach based on reconfigurable magnetic resonant structures is proposed to achieve high energy efficiency and low volt-amp ratings. This basic principle is to create more than one efficiency–load curve. The WPT system is controlled to be operated within the top regions of the energy efficiency curves of the reconfigurable circuits so that high energy efficiency can be achieved over a very wide load range. The principle of this new approach is explained with an analysis and verified with practical measurements.**

***Index Terms*—Reconfigurable wireless power systems, wireless power transfer (WPT), magnetic resonance.**

I. Introduction

WIRELESS power transfer (WPT) has already reached commercialization stage in the inductive pickup systems in the manufacturing facilities of clean rooms [1] and portable consumer electronics such as mobile phones [2], [3] over the last decade. Active research has recently been extended to static and dynamic charging of electric vehicles [4]–[6] and medical implants [7]–[9]. Among various WPT applications, batteries are the most common load type. In the battery charging process, the load power as well as the equivalent load resistance of the charging system are changing in a relatively low speed (compared to the responding speed of the charging system). However, the power transfer efficiency of a WPT system is highly dependent on the load resistance. Therefore, in order to obtain a high power transfer efficiency for the whole or most part of the load range, the load resistance of a WPT system should be transformed to the optimum load resistance of the system. Many works have been done on this subject. Generally, there are at least four commonly used methods which can realize load resistance transformation.

A. Using DC–DC Converters for Altering Load Impedance [10]–[20]

In the receiver circuit, the receiver coil picks up the coupled high-frequency voltage which is usually fed to a rectifier. After the rectifier, dc–dc power converters have been used in various ways to alter the equivalent load resistance for optimal energy efficiency. A large number of papers are based on this approach because of the flexibility in controlling the power converter to alter the equivalent impedance of the load.

In [10] and [11], a boost–buck converter is used after the rectifier circuit for impedance matching. These two projects use S-matrix analysis. The impedance matching method is based on matching the input impedance of the WPT system with the input source impedance based on the maximum power transfer theorem, which results in losing at least 50% of the input power from the ac power source. On the other hand, dc–dc converters have been used to maximize the overall energy efficiency based on the maximum energy efficiency method. In [12], a buck–boost converter (which is capable of transforming a load resistance to a value either larger or smaller than the practical value) has been adopted for maximum energy efficiency tracking (MEET) without any wireless communication unit. Using a secondary closed-loop control to regulate the output voltage for the load, Zhong and Hui [12] search for the minimum input power condition for the transmitter circuit for any given output power. This operation automatically guarantees the maximum energy efficiency for the WPT system. Based on this concept, the search process in [12] is replaced with a feedback control in order to speed up the dynamic response in [13]. Another approach for MEET based on the uses of a boost converter and a wireless feedback system has also been proposed in [14]. This structure was later used in [15] for charging a battery. Based on a three-coil WPT structure, dc–dc converters are used in [16] and [17] to alter and amplify the quality factor of the reflected impedance in order to maximize the overall energy efficiency. Since the optimal energy efficiency conditions change with the coupling coefficient k, a recursive least square filter is used to determine the instantaneous value of k and a buck converter is adopted after the diode rectifier in [18] to locate the maximum energy efficiency conditions. If space in the receiver module is

Manuscript received February 24, 2017; revised May 11, 2017 and June 20, 2017; accepted July 16, 2017. Date of publication August 31, 2017; date of current version March 5, 2018. This work was supported by the Hong Kong Research Grant Council under GRF Project 17255916 and the Fundamental Research Funds for the Central Universities. Recommended for publication by Associate Editor J. Acero. *(Corresponding author: S. Y. (Ron) Hui.)*

Wenxing Zhong was with the Department of Electrical and Electronic Engineering, The University of Hong Kong, Pokfulam, Hong Kong. He is now with the Department of Electrical Engineering, Zhejiang University, Zhejiang 310027, China (e-mail: wxzhong@zju.edu.cn).

S. Y. R. Hui is with the Department of Electrical and Electronic Engineering, The University of Hong Kong, Pokfulam, Hong Kong, and also with the Imperial College London, London, SW7 2AZ, U.K. (e-mail: ronhui@eee.hku.hk).

Color versions of one or more of the figures in this paper are available online at http://ieeexplore.ieee.org.

Digital Object Identifier 10.1109/TPEL.2017.2748161

not an issue, an auxiliary measurement coil has been added in the receiver side [19] to provide the phase information of the induced voltage so that the secondary control can tune the receive side and control the equivalent load resistance to the optimal value. A wireless communication unit is needed for providing load information to the transmitter circuit for MEET operation. Recently, a new approach has been reported in [20], which involves the combined uses of an intermediate capacitor in the receiver circuit as a power flow indicator, hysteresis-controlled switching actions of a shunt decoupling switch in the receiver circuit to regulate the dc voltage of the intermediate capacitor, and the charging and discharging times of the decoupling switch detected on the primary side for closed-loop control. This is a primary- or transmitter-side control method, which can eliminate the requirements for precise information of the mutual coupling and wireless communication unit.

B. Using Passive Circuits for Impedance Matching [21]–[27]

Besides actively switched power converters, using passive resonant circuits or coils for impedance matching is another common approach. Different placements of the passive circuits have been suggested. An *LCC* circuit has been inserted in the transmitter circuit in [21], while an *LC* circuit is placed after the high-frequency rectifier on the receiver circuit in [22] and before the rectifier in [23]. In the four-coil WPT systems [24], [25], two coupled coils are placed the transmitter and receiver resonators in order to provide two extra mutual inductance terms for impedance matching with the impedance of the input power source. Manual adjustments of the coupled coil locations with respect to their coupled resonators can be made to maximize the power transfer. The techniques in [21]–[25] are based on the maximum power transfer theorem that requires impedance matching with the power source. This approach, as explained previously, suffers relatively high power loss in the power source resistance and is, therefore, suitable only for very low power applications (say $<$ 1 W). Of course, an *LC* resonator can be used as a third coil in the WPT system, as demonstrated in [26] and [27]. The relay resonator can play a role in enlarging the relay resonator current and its flux linkage with the receiver coil while reducing the transmitter coil current and the conduction loss in the transmitter circuit.

C. Reconfigurable Resonant Circuits for Impedance Matching [28]–[31]

Reconfigurable resonant circuits usually involve a switchable capacitor array or inductive coil or their combinations for altering the resonant frequency in order to achieve the optimal energy efficiency conditions in the events of load changes. Examples of using switchable capacitor arrays and capacitive matrix are given in [28] and [29], respectively, while Lee *et al*. [30] use a set of switchable coils. In [31], the use of a combination of switchable capacitors and inductors is proposed. Using reconfigurable resonant circuits have both advantages and disadvantages. On one hand, a higher number of switchable capacitors or inductors provides a wide discrete steps of changes in the resonant frequency. One the other hand, it involves a corresponding increase in the circuit complexity and size of the circuits because many switches and their corresponding driving circuits and control are required. However, if this method can be modified to use only one or two switches, it may offer an attractive solution to some application where high efficiency operation is needed for a wide range of load. This aspect forms an important part of this project.

D. Using Variable Operating Frequency [32]–[34]

By changing the operating frequency with the load resistance, a higher efficiency can be achieved. Examples are provided in [32]–[34]. However, it has been pointed out in [12] that the efficiency improvement is obvious only when the load resistance is much larger than the optimum load resistance. Moreover, the maximum efficiency for a given load by shifting the operating frequency to non-resonant frequency will be much lower than the maximum efficiency of the system. The reason is that when the system is operating at non-resonant frequency, some reactive power will be delivered to the secondary side and reactive power will only cause power loss.

In this project, a reconfigurable structure which combines the functions of a matching network and the transformer mechanism such as the technique used in a three-coil system is investigated. No additional coil is used because the different portions of the same receiver coils are used to realize the transformer action. The idea is to design the optimal efficiency ranges of two or more resonant tanks' characteristics so that their combined high-efficiency range covers a very wide range of the load. Near maximum efficiency can be achieved for a load resistance in the range roughly from 1/10 to 20 times of the optimum load resistance. In this paper, the following steps are carried out: 1) the impedance transformation network is studied first; 2) a new reconfigurable receiver coil structure is proposed for extending high-energy-efficiency operation over very wide load range; and 3) a novel WPT system combining reconfigurable receiver coil structure and impedance transformation network is proposed for maximizing both the energy efficiency and power transfer for any arbitrary load range. The proposed WPT approach has been tested in a 10-W experimental prototype. Practical results are included to confirm the validity of the proposal.

II. Optimum Load Resistance and Efficiency Variations of a Two-Coil WPT Systems

Fig. 1 shows the circuit model for a two-coil WPT system. The operating frequency is chosen to be equal to the resonant frequency of these two *L–C* resonators, i.e., $f = \frac{1}{2\pi\sqrt{L_P C_P}} = \frac{1}{2\pi\sqrt{L_S C_S}}$. Thus, the system can be expressed with (1) and (2).

$$R_P \mathbf{I_P} + j\omega M_{PS} \mathbf{I_S} = V_S \tag{1}$$

$$j\omega M_{\mathrm{PS}} \mathbf{I_P} + (R_S + R_L)\, \mathbf{I_S} = \mathbf{0} \tag{2}$$

where V_S is the root-mean-square (RMS) value of the input sine-wave voltage. $\mathbf{I_P}$, $\mathbf{I_S}$ are the phasors of the current in the primary coil and the secondary coil, respectively. R_P and R_S are the parasitic resistances of the resonator, as shown in Fig. 1.

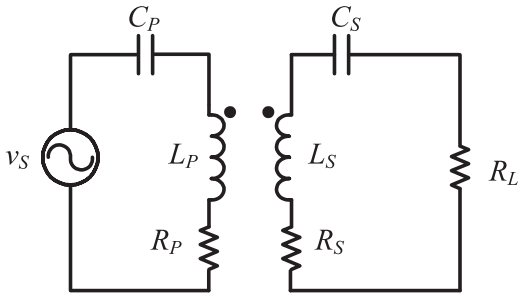

Fig. 1. Circuit model of a two-coil WPT system.

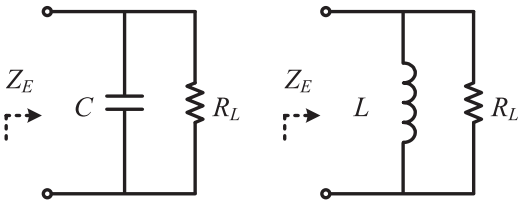

Fig. 2. Parallel an inductor or a capacitor with the load.

In [12], the optimum load resistance of a two-coil WPT system to reach a maximum energy efficiency is expressed as

$$R_{L\_\mathrm{OPT}} = R_S \left(\sqrt{1 + \frac{\omega^2 M_{PS}^2}{R_P R_S}} \right). \tag{3}$$

For the load resistance located in a small range centered with this optimum value, the power transfer efficiency of the system can be maintained relatively high. However, when the actual load resistance is far from this range, the energy efficiency of the system will be degraded. This will be clearly shown in the following analysis and experiments.

III. Using Inductor or Capacitor to Transform Load Resistance Larger Than the Original Optimum Value

In radio-frequency (RF) applications, *L–C* networks are commonly used for impedance matching since the load impedance (or resistance) can be transformed and match to the source impedance by properly connecting inductors and capacitors between the source and the load. This is normally termed narrowband matching which means that it only works for a narrow designated frequency band.

For power applications which are usually operating at a much lower frequency than RF, the impedance transformation mechanism behind matching networks is not to match the load impedance to the source impedance. Instead, the matching networks are used to transform the load impedance to match the optimal load value at which maximum energy efficiency can be achieved.

For paralleling an inductor or a capacitor with the load as shown in Fig. 2, the equivalent impedance can be expressed as

$$Z_E = \frac{R_L}{1 + R_L^2/X^2} + j\frac{X R_L^2}{X^2 + R_L^2} \tag{4}$$

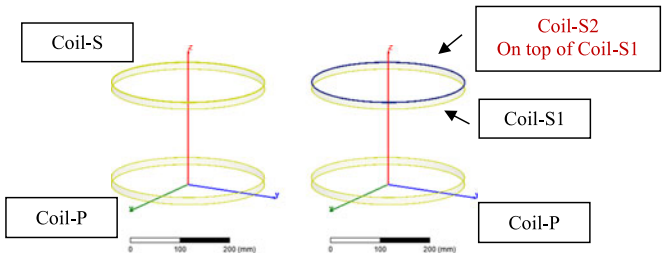

Fig. 3. Receiver coil is split into two coils.

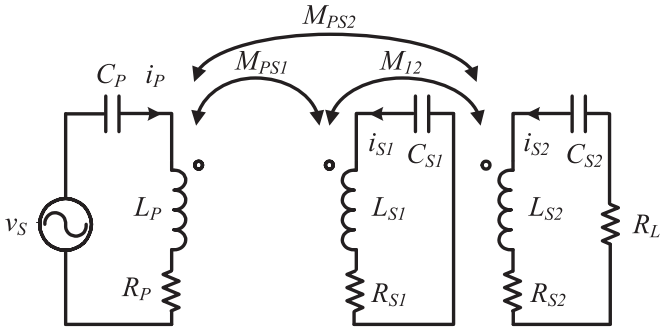

Fig. 4. Schematic of the system with receiver coil split into two.

where $X = \omega L$ or $\frac{1}{\omega C}$. Then the equivalent load resistance is

$$R_{EL} = \frac{R_L}{1 + R_L^2/X^2}. \tag{5}$$

Therefore, the equivalent load resistance can be transformed to be smaller than the actual load resistance. If this equivalent load resistance is equal to the optimum load resistance, the maximum efficiency of the system can be achieved by compensating this extra reactance induced by the capacitor. Thus, by setting

$$R_{EL} = R_{L\_\mathrm{OPT}} \tag{6}$$

the required reactance can be worked out with following equation:

$$X = \pm R_L \sqrt{\frac{R_{L\_\mathrm{OPT}}}{R_L - R_{L\_\mathrm{OPT}}}}. \tag{7}$$

IV. Using Receiver Coil Splitting to Transform Equivalent Load Resistance Smaller Than the Optimum Value

As shown in Fig. 3, the receiver coil, i.e., Coil-S, is split into two coils Coil-S1 and Coil-S2, while the transmitter coil, i.e., Coil-P, is unchanged. Fig. 4 shows the circuit model of the three-coil WPT system where, R_P is the resistance in the primary loop, which normally includes the source resistance of the power source and the parasitic resistance of the coil and the compensated capacitor; R_{S1} and R_{S2} are the parasitic resistance in respective current loops; R_L is the load resistance; L_P, L_{S1}, L_{S2}, C_P, C_{S1}, C_{S2} are the respective self-inductance of the coils and the compensated capacitance; M_{PS1} and M_{PS2} are the mutual inductance between the primary coil and the first splitting coil and the second splitting coil, respectively; M_{12} is the mutual inductance between two splitting coils.

TABLE I
PARAMETERS OF THE WPT SYSTEM USED FOR SIMULATIONS AND EXPERIMENTS

Radius of windings	155 mm
Number of turns	11
Layers of the wire	1
Structure of the wire	Ø 0.12 mm × 50 strands Outer Ø 1.2 mm
Self-inductance	91.25 μH
Parasitic resistance	0.394 Ω ($Q = 146$; 100 kHz)
Distance between the transmitter and receiver coils	85 mm ($k = 0.179$)

If the loaded coil is Coil-S2 in the three-coil system, there are two possible paths for power transfer, i.e., "Coil-P to Coil-S2" and "Coil-P to Coil-S1 to Coil-S2". Assume that Coil-S1 has most of the turns of the original coil and Coil-S2 has a small portion of the turns of the original coil, e.g., 1 turn. Then the first power path can be neglected because the mutual inductance M_{PS2} will be much smaller than the mutual inductance M_{PS1} and M_{12}. So most of the power will be delivered to Coil-S2 through the second power path in which Coil-S1 performs as a relay coil. Also, the power loss in Coil-S2 is negligibly small because the resistance of Coil-S2 is very small compared with a normal load resistance. Assuming the coils are resonant at the operating frequency, the simplified circuit equations of the system without considering the first power path and the power loss in Coil-S2 can be expressed as follows:

$$R_P\mathbf{I_P} + j\omega M_{PS1}\mathbf{I_{S1}} = V_S \tag{8}$$

$$j\omega M_{PS1}\mathbf{I_P} + R_{S1}\mathbf{I_{S1}} + j\omega M_{12}\mathbf{I_{S2}} = \mathbf{0} \tag{9}$$

$$j\omega M_{12}\mathbf{I_{S1}} + R_L\mathbf{I_{S2}} = \mathbf{0}. \tag{10}$$

The reflected load resistance in Coil-S1 is

$$R_{L\_S1} = \frac{\omega^2 M_{12}^2}{R_L}. \tag{11}$$

Setting

$$R_{L\_S1} = R_{L\_\mathrm{OPT}} \tag{12}$$

then

$$M_{12} = \frac{\sqrt{R_L R_{L\_\mathrm{OPT}}}}{\omega}. \tag{13}$$

Therefore, the smaller the R_L is, the smaller the required M_{12} should be in order to maximize the power transfer efficiency. Equation (13) provides an approximate optimal M_{12}, which shows that the receiver coil splitting is indeed able to convert the load resistance to another value.

A case study is provided to prove the receiver coil splitting will have a smaller optimum load resistance. The study is based on two identical coils with parameters listed in Table I. The coupling coefficient (k) between two coils is about 0.179. Each of the coils has a single layer 11-turn (axial arrangement) structure, as shown in Fig. 5. In this study, the receiver coil is split into two coils to form two selectable coil resonators with resonant capacitors. The receiver coil is split into two as shown in

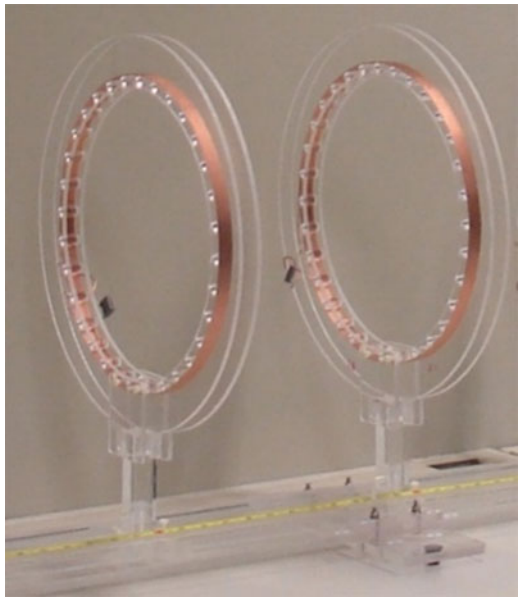

Fig. 5. Coils used for simulation study and experiments.

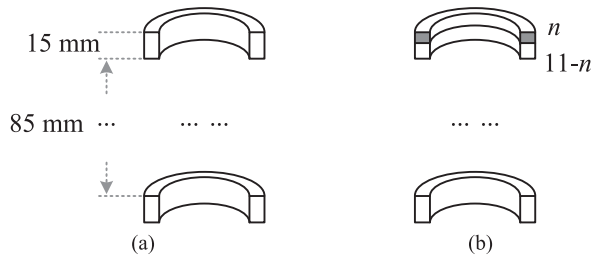

Fig. 6. (a) Original two-coil system with the bottom coil as the transmitter coil; (b) receiver coil split into two coils.

Fig. 6. The upper split-coil has *n* turns ($n = 1, 2, \ldots, 10$), and thus, the lower one has ($11 - n$) turns. The operation frequency is set at 100 kHz. At this frequency, the ac resistance of the coils is negligibly small as reflected in the practical measurements (about 6% of the dc resistance). Therefore, a simplification is made that the resistance of the split coils is proportional to the number of turns. The upper coil is connected to the load.

The general equations for the three-coil system shown in Fig. 6 are

$$(R_P + jX_P)\mathbf{I_P} + j\omega M_{PS1}\mathbf{I_{S1}} + j\omega M_{PS2}\mathbf{I_{S2}} = V_S \tag{14}$$

$$j\omega M_{PS1}\mathbf{I_P} + (R_{S1} + jX_{S1})\mathbf{I_{S1}} + j\omega M_{12}\mathbf{I_{S2}} = \mathbf{0} \tag{15}$$

$$j\omega M_{PS2}\mathbf{I_P} + j\omega M_{12}\mathbf{I_{S1}} + (R_{S2} + R_L + jX_{S2})\mathbf{I_{S2}} = \mathbf{0} \tag{16}$$

where $X_{P,S1,\mathrm{or}\,S2} = \omega L_{P,S1,\mathrm{or}\,S2} - \frac{1}{\omega C_{P,S1,\mathrm{or}\,S2}}$. In order to maximize the efficiency of the given system, C_{S1}, C_{S2}, and R_L can be optimized.

The number of turns of the upper split coil (connected to the load) is changed from 1 to 10 in a step-by-step manner as shown

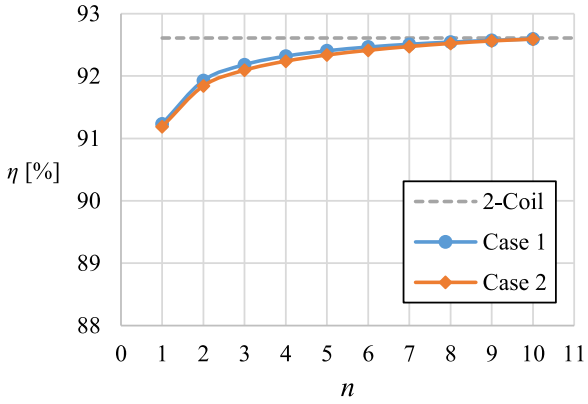

Fig. 7. Maximum efficiency versus n for the two-coil, Case 1 and Case 2, configurations.

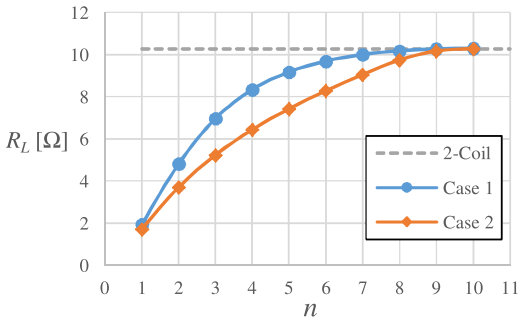

Fig. 8. Optimum load resistance versus n for the two-coil, Case 1 and Case 2, configurations.

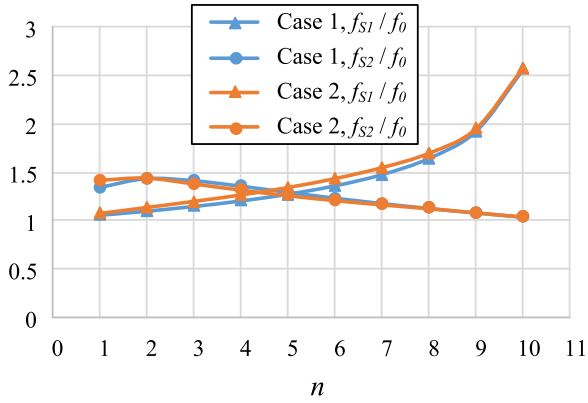

Fig. 9. Individual resonant frequency of the split coil resonators normalized at the operating frequency of 100 kHz.

in Fig. 6. The optimization results are shown and labeled as Case 1 in Figs. 7–9.

Case 2 is the optimization under the constraint that C_{S1} in series of C_{S2} will meet the required capacitance for the whole receiver coil to resonate at the operating frequency (100 kHz). An important feature of this research idea is to enable the WPT system to operate flexibly in either two-coil mode or three-coil mode. The schematic of the proposed system is shown in Fig. 10 and will be analyzed in the next section. Therefore, the conditions of the optimization of Case 1 and Case 2 can be

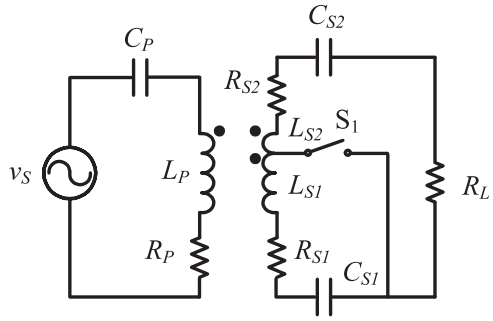

Fig. 10. Proposed WPT system that can operate either in the three-coil mode or in the two-coil mode.

expressed mathematically as

$$\text{Case 1}: \quad \max: \eta = \mathrm{f}(C_{S1}, C_{S2}, R_L) \tag{17}$$

$$\text{Case 2}: \quad \max: \eta = \mathrm{f}(C_{S1}, C_{S2}, R_L) \tag{18}$$

$$\text{with constraint: } \frac{1}{\omega C_{S1}} + \frac{1}{\omega C_{S2}} = \omega L_S \tag{19}$$

where L_S is the self-inductance of the whole secondary coil. For each n, a set of optimum values for C_{S1}, C_{S2}, and R_L will be determined.

Fig. 7 shows the maximum efficiency curves versus n under the two cases. It is noted that the efficiency curves of the two cases of coil splitting are very similar. When n is small in the two cases of coil splitting, there is only a small efficiency drop (of about 1.4% when $n = 1$) when compared with the maximum efficiency of the original two-coil structure. This observation on splitting receiver coil is consistent with the previous results [30] that a three-coil system with split transmitter coils could have nearly the same maximum efficiency as that of the original two-coil system under certain conditions, regardless of the ratio of the coil splitting.

Fig. 8 shows the optimum load resistance value versus n for the two cases. The minimum R_{L_OPT} becomes 1.7 Ω when $n = 1$, while the optimum load resistance of the original two-coil system is 10.3 Ω. When n becomes larger, the optimum load value of the three-coil system approaches the optimum load value of the two-coil system. Therefore, splitting the receiver coil does have the ability to shift the optimum load resistance to a smaller value. This interesting feature provides a useful mechanism to achieve high energy efficiency over a wide load range.

As mentioned previously, paralleling an inductor or a capacitor with the load can shift the optimum load resistance to a larger value only. Therefore, for some applications in which the real load resistance is smaller than the optimum load resistance of the designed two-coil system, splitting receiver coil is a practical and feasible solution with negligible efficiency degradation as predicted in Fig. 7.

Fig. 9 shows the variations of the per-unit ratios of the resonant frequencies of the split receiver coils with the optimized compensated capacitance (f_{S1} for the upper split coil resonator and f_{S2} for the lower split coil resonator) using the operating frequency of the system f_0 (i.e., 100 kHz) as the base value.

It can be observed that the two curves of f_{S1}/f_0 almost overlap for Case 1 and Case 2. Similarly, the two curves of f_{S2}/f_0 also overlap for the two cases. The overlaps of these two sets of curves indicate that the resonant frequencies of the splitting the receiver coils with different turns ratio do not equal to the operating frequency of the system except at the two extreme points. This feature is different from the operation principle of a two-coil system. The reason for this difference is that splitting the receiver coil resonator into two-coil resonators forms a higher order resonant system. Therefore, the individual resonant frequency is not going to dominate the power transfer efficiency of the system.

From Figs. 7 and 9, it can be seen that the maximum efficiency and the individual resonant frequency of the split coils under Case 1 and Case 2 are nearly the same. As shown in Fig. 8, the range of the optimum load resistances for these two cases are also the same, i.e., from about 1.7 to 10.3 Ω (which is the optimum load resistance for the two-coil system). But the curve of the optimum load resistance as a function of n in Case 2 is much more linear than that of Case 1.

In this study, the upper split coil is connected to the load. In principle, the lower split coil can be connected to the load if desired. Calculations have been done on these two alternative load arrangements. The results are almost the same. For example, if the load is connected to the upper coil and $n = 1$, the optimum load resistance, the capacitance C_{S1} and C_{S2} in Case 1, and the maximum efficiency are, respectively, 1.95 Ω, 29.45 nF, 1.255 μF, and 91.23%. If the load is connected to the lower coil and $n = 10$ (loaded coil has one turn), the optimum load resistance, the capacitance C_{S1} and C_{S2} in Case 1, and the maximum efficiency are, respectively, 1.88 Ω, 28.95 nF, 1.206 μF, and 91.32%.

V. New Reconfigurable Topologies for Maximizing Efficiency and Power Over Wide Load Range

A. Extending High-Efficiency Region to the Low Load Resistance Range

The analysis presented in the last section shows that splitting the receiver coil can achieve a maximum efficiency similar to that of the original two-coil system, but the optimal load resistance value can be transferred to a much lower value. However, either two-coil or three-coil structure can only maintain high efficiency within a narrow load resistance range. Therefore, a reconfigurable receiver circuit structure as shown in Fig. 10 is proposed to enable the WPT system to operate either in two-coil mode or three-coil mode in order to widen the high-efficiency operating range. The receiver coil is dual tapped and a switch is added to switch the secondary circuit to operate in two-coil mode or three-coil mode. When the switch S_1 is turned on, a three-coil system is formed and the load is connected to L_{S2} (the small coil in this design). Under this condition, L_{S1} (the large coil) and C_{S1} form a coil resonator and acts as a repeater. Thus, the system will operate in the three-coil mode. When the switch S_1 is turned off, the receiver circuit is reverted to a two-coil system. The whole receiver coil will resonate with the series-connected resonant capacitors C_{S1} and C_{S2}. For battery charging applications, the mode switching time will not affect the performance of the whole system. Therefore, low-speed low-cost relay or bidirectional switch could be used for mode switching.

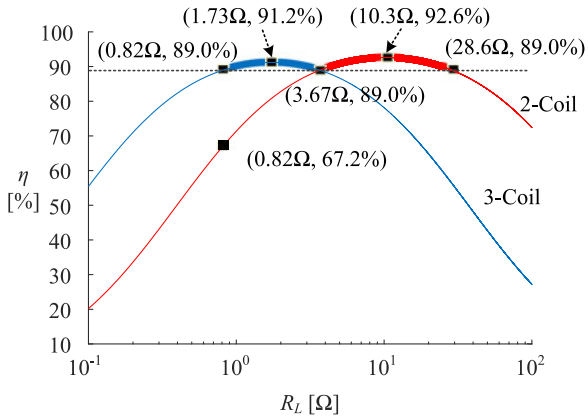

Fig. 11. Efficiency curves of the three-coil and two-coil modes ($k = 0.179$).

Fig. 11 shows the energy efficiency curves of the two-coil and three-coil configurations of the proposed system as a function of the load resistance. It should be noted that the x-axis uses a logarithmic scale for the load resistance value. The top parts of the two energy efficiency curves are highlighted in blue color for the three-coil mode and red color for the two-coil mode. The mode switching will be conducted at the crossover load resistance point of 3.67 Ω. The three-coil mode can be used when the load resistance is less than 3.67 Ω, while the two-coil mode should be used when the load resistance exceeds 3.67 Ω.

Assuming the design target is to achieve efficiency not lower than 89% for all load resistance, the three-coil mode will extend the minimum load resistance from 3.67 to 0.82 Ω. If the application needs to operate with 0.82 Ω and the traditional two-coil system is used, the efficiency is only 67.2%. By using three-coil mode, the efficiency improvement is 22.2%.

It should be noted that this case study is a general analysis. It shows that the three-coil mode is able to extend the high-efficiency load resistance range to much lower load resistance values.

B. Extending High-Efficiency Region to the High Load Resistance Range

If the practical load resistance is much larger than the optimum load resistance of the two-coil system, high efficiency can be extended to the high load resistance range by using a parallel a capacitor with the load resistance as analyzed in Section III. A second reconfigurable receiver circuit is hereby proposed here and shown in Fig. 12. One additional capacitor C_{LP} is connected in parallel with the load and another capacitor C_{S1P} is added to compensate the extra reactance caused by C_{LP}. Two more low-speed switches are added for mode switching. Now, the system has the following three operation modes:

1) three-coil mode (S_1 on; S_2 and S_3 off);
2) two-coil mode (S_1 off; S_2 and S_3 off)
3) two-coil with parallel capacitor mode (S_1 off; S_2 and S_3 on)

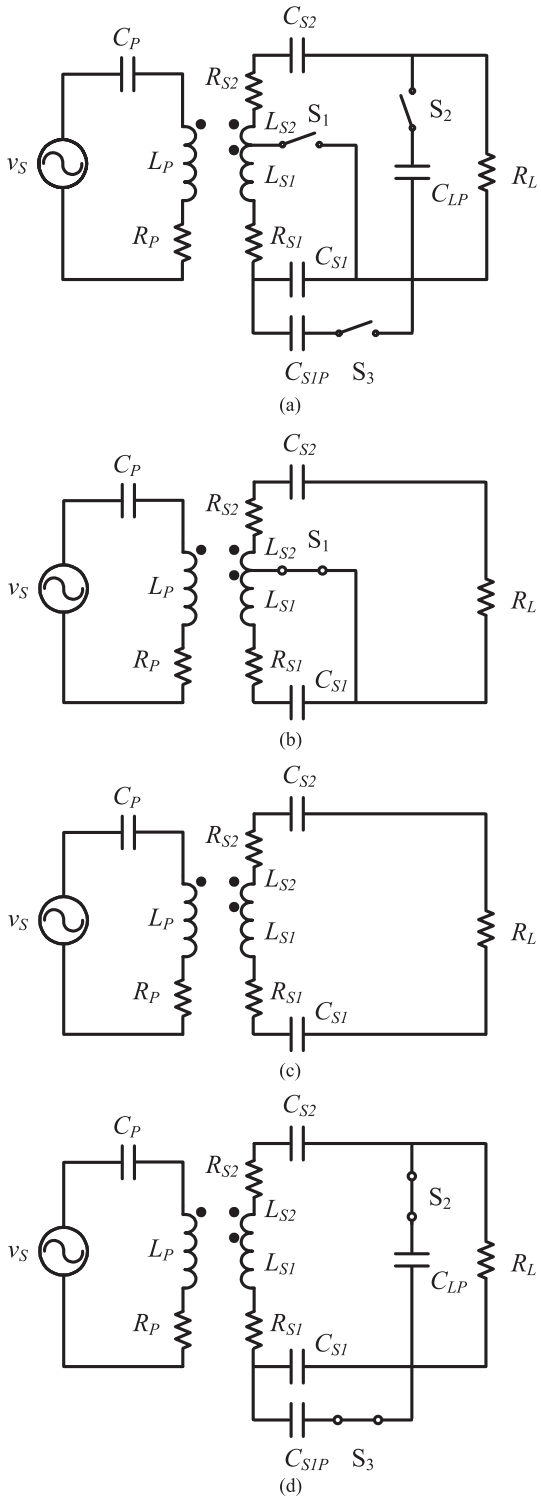

Fig. 12. (a) Proposed WPT system with three reconfigurable topologies and the equivalent topologies under the three operating modes: (b) three-coil mode, (c) two-coil mode, and (d) two-coil mode with parallel capacitor mode.

The third mode is the two-coil structure with a parallel capacitor, and it enables high efficiency to be extend over the optimum load resistance point of the original two-coil system. The efficiency curves under the three operating modes of this reconfigurable receiver circuit as a function of the load resistance

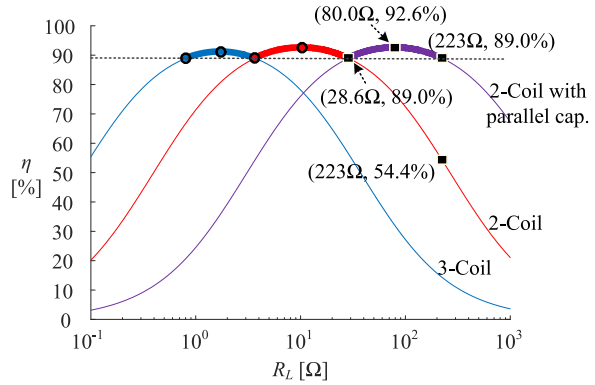

Fig. 13. Efficiency curves of the three-coil, two-coil, and two-coil modes with parallel capacitor modes($k = 0.179$).

is shown in Fig. 13. The load resistance range with efficiency exceeding 89% for the original two-coil system is from 3.67 to 28.6 Ω (i.e., **7.8** times the minimum load resistance). By using the proposed circuit, the new load resistance range with efficiency exceeding 89% is from 0.82 Ω to 223 Ω (i.e., **272** times the minimum load resistance). The load resistance range is $272/7.8 = \mathbf{35}$ times larger.

For the second reconfigurable receiver circuit, the optimum values of C_{S1} and C_{S2} are the same 28.5 nF and 1.13 μF as those for the system in Fig. 10 and can be worked out by maximizing the efficiency of the three-coil mode, as described in (18) and (19). Then for the third operation mode, a target load resistance should be determined. For the system studied in the paper, the efficiency of the original two-coil mode maximizes at 10.3 Ω load resistance and achieves 89% higher in the load resistance range between 3.67 and 28.6 Ω, as shown in Fig. 11. Therefore, one may expect that the efficiency curve of the third operating mode will intersect with the efficiency curve of the two-coil mode at 28.6 Ω. This means the efficiency of the third operating mode will maximize at about $28.6 \times 28.6/10.3 \approx 80\,\Omega$. According to (5) and (6), the value of C_{LP} (which can transfer 80 Ω to the optimum load resistance) could be obtained as 51.8 nF. Then the whole secondary circuit in the third operating mode should be resonant at the operating frequency, i.e., the imaginary part of the impedance should equal to zero which can be expressed as

$$\omega L_2 - \frac{1}{\omega C_{S2}} - \frac{1}{\omega\left(C_{S1} + C_{S1P}\right)} + \frac{X_{LP} R_L^2}{{X_{LP}}^2 + R_L^2} = 0. \tag{20}$$

By solving (20), C_{S1P} can be obtained as 26.1 nF.

C. VA Rating Minimization or Power Maximization

Apart from the efficiency improvement, the required VA rating of the system can also be minimized by using the proposed reconfigurable WPT system for a given output power, when compared with the original two-coil system. Here, the VA rating means the product of the required input voltage and the primary coil current for a given output power. Fig. 14 shows the required input voltage for 10 W output. The bolded curves

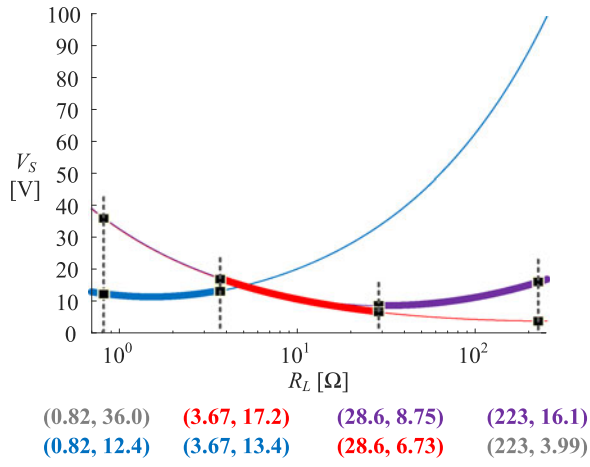

Fig. 14. Required input voltage for 10 W output (blue: three-coil mode; red: two-coil mode; purple: two-coil with parallel capacitor mode).

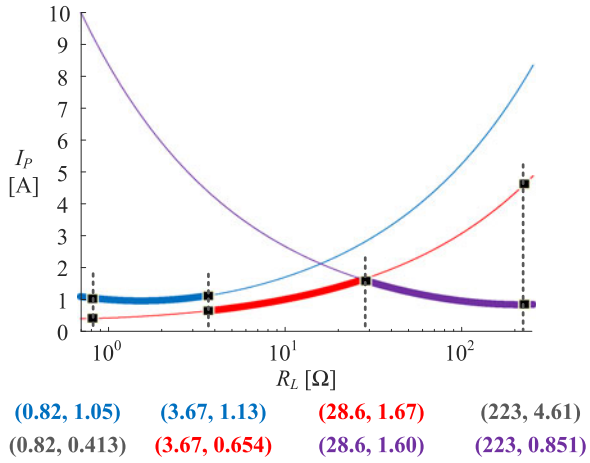

Fig. 15. Required primary coil current for 10 W output (blue: three-coil mode; red: two-coil mode; purple: two-coil with parallel capacitor mode).

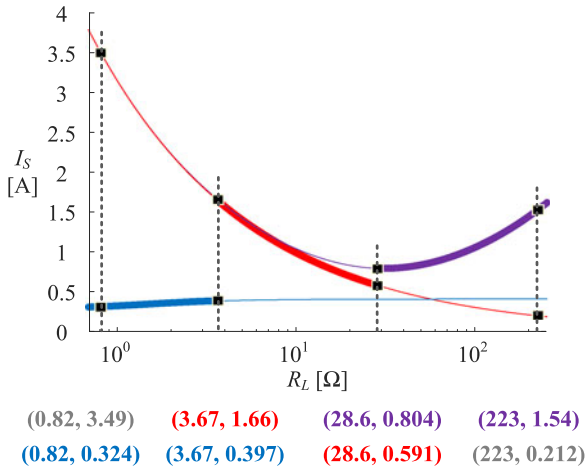

Fig. 16. Required secondary coil current for 10 W output (blue: three-coil mode; red: two-coil mode; purple: two-coil with parallel capacitor mode).

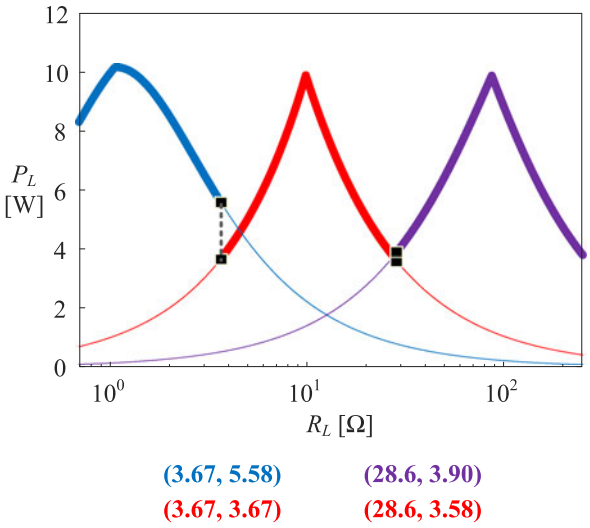

Fig. 17. Maximum output power with the constraint of maximum coil current equals to 1 A output (blue: three-coil mode; red: two-coil mode; purple: two-coil with parallel capacitor mode).

are the operating region for the reconfigurable WPT system. It can be seen that, by switching the operating mode to stay in the region with the low input voltage requirements, this WPT system can be operated in a range of 6.7–16 V for the whole load resistance range of interest. This advantageous feature will not only minimize the voltage rating for the whole system but also avoid the primary dc–dc converter (feeding the inverter) or the inverter to operate with an extremely small duty cycle.

Current rating is another critical design parameter because it determines the size of the wire used and accordingly the copper cost. Figs. 15 and 16 show the required current in the primary coil and secondary coil for 10 W output, respectively. For the two-coil with parallel capacitor mode, the secondary coil current means the current in the larger coil which takes up most of the copper in the secondary side. The current rating for both the primary and secondary coil of the universal system are about 1.67 A.

Figs. 14–16 show not only the low VA rating requirements of the system but also the points of mode switching. Mode switching can thus be easily achieved by monitoring the equivalent load resistance. Minimizing the VA rating of the system for a given output power is equivalent to maximizing the output power within given voltage and/or current constraint. Fig. 17 shows the output power of the reconfigurable WPT system with 1 A limitation for the coil current. It is clear that this WPT system enables the use of the respective maximum power region of all three operating modes.

D. *Effect of Coupling Variation*

The aforementioned analysis on the proposed structure is based on a fixed mutual coupling coefficient. In practice, the transmitter coil and the receiver coil may not be placed in the same relative positions. Also, there could be misalignment issue in many applications. Therefore, one can select the worst-case situation (with the lowest mutual coupling coefficient) in the aforementioned analysis and design procedure.

Two simulation studies are carried out to investigate the effects due to coupling variation. The first simulation assumes the coupling coefficient (k) is reduced by half from 0.179 to 0.0895.

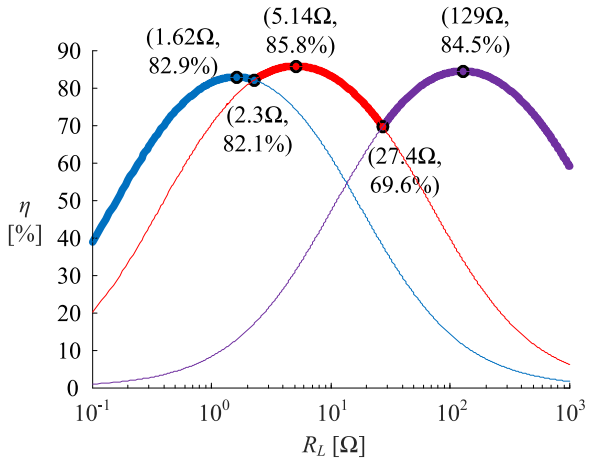

Fig. 18. Energy efficiency curves of the proposed three-coil-mode WPT system when k is reduced by half from 0.179 to 0.0895.

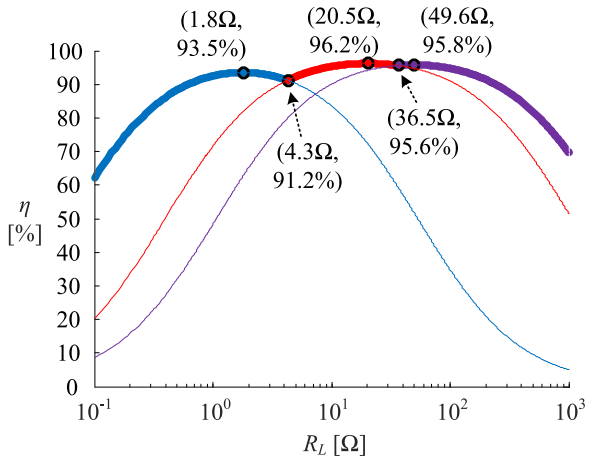

Fig. 19. Energy efficiency curves of the proposed three-coil-mode WPT system when k is doubled from 0.179 to 0.358.

The energy efficiency versus load resistance plot is shown in Fig. 18. It can be seen that the reconfigurable WPT system can still be operated at the highest efficiency regions of the 3 configurations, although these efficiency values are lower than those in Fig. 13, which has a higher k of 0.179.

The second simulation assumes k to be doubled from 0.179 to 0.358. The corresponding result is shown in Fig. 19. Again, the high-efficiency portions of the efficiency curves can be used over a wide load resistance range. Because of a higher k, the energy efficiency values in Fig. 19 are higher than those in Fig. 13.

E. Generalization of the Principle

Theoretically and practically, this high-efficiency load range can be further extended. As mentioned previously, if the number of turns for the small split coil in the three-coil mode is further reduced, e.g., 0.5 turn, the minimum load resistance can be smaller. However, in this case study, the total number of turns of the coils is 11, therefore, if coils with more turns

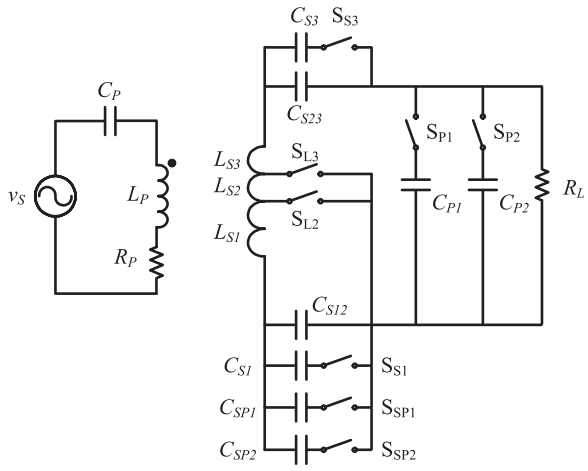

Fig. 20. Reconfigurable WPT system with five operating modes.

are used, the minimum load resistance could be much smaller than the optimum value of the original two-coil system. Because the ratio of the number of turns between the small coil and the large coil will be much smaller. For larger load resistance, the value of the parallel capacitor, i.e., C_{LP}, can be changed to transform the load resistance to the optimum value as expressed in (3). Therefore, the high-efficiency load resistance can be theoretically extended to any given value. Fig. 20 shows the schematic of a universal WPT system with larger load resistance range and following five operating modes:

1) For $R_{\min} < R_L < R_1$: three-coil mode with L_{S3} connected to load (S_{L3}, S_{S3} on; S_{L2}, S_{S1}, S_{SP1}, S_{SP2}, S_{P1}, S_{P2} off).
2) For $R_1 < R_L < R_2$: three-coil mode with $L_{S3} + L_{S2}$ connected to load (S_{L2}, S_{S1} on; S_{S3}, S_{L3}, S_{SP1}, S_{SP2},S_{P1}, S_{P2} off).
3) **For $R_2 < R_L < R_3$: two-coil mode (S_{S3} on; S_{L3}, S_{L2}, S_{S1}, S_{SP1}, S_{SP2}, S_{P1}, S_{P2} off).**
4) For $R_3 < R_L < R_4$: two-coil mode with $C_{P1} + C_{P2}$ parallel with load (S_{S3}, S_{P1}, S_{P2}, S_{SP1} on; S_{L3}, S_{L2}, S_{S1}, S_{SP2} off).
5) For $R_4 < R_L < R_{\max}$: two-coil mode with C_{P1} parallel with load (S_{S3}, S_{P1}, S_{SP1}, S_{SP2} on; S_{L3}, S_{L2}, S_{S1}, S_{P2} off).

Mode 3 is the original two-coil system. Therefore, $R_{\min} < R_1 < R_2$ are smaller than the optimum load resistance of the original two-coil system and $R_3 < R_4 < R_{\max}$ are larger than the optimum value. Capacitors C_{S1}, C_{SP1}, C_{SP2}, and C_3, C_{S23} are not necessarily connected in parallel. Series connection might also work as long as the capacitance meet the compensation requirement for each of the modes. Also, inductors might also be used for compensation in order to extend the load resistance to even larger value. However, in practical battery charging applications, the load resistance is normally in a range of 1 to 200 Ω. Therefore, it is not necessary to consider an extremely large load resistance.

While the proposed idea is demonstrated in a series-series resonant WPT system in this paper, it should be noted that it

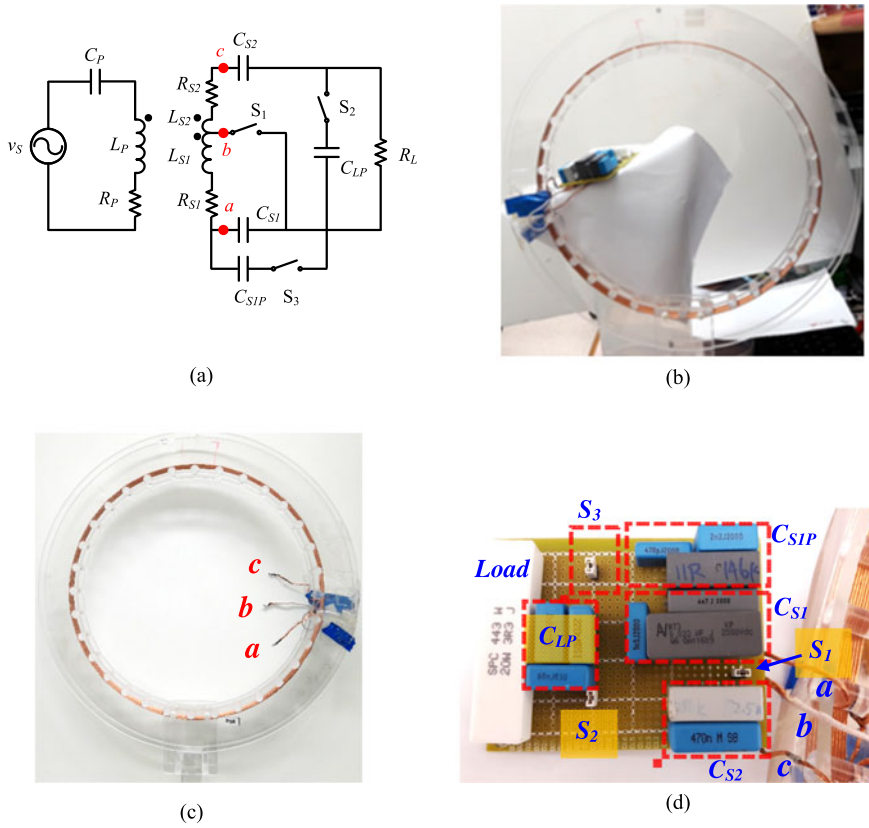

Fig. 21. Setup of the proposed system. (a) Schematic of the proposed system. (b) Setup of the secondary side. (c) Receiver coil splitting. (d) Secondary-side circuit.

TABLE II
PARAMETERS OF THE SPLITTING COILS AND THE CAPACITORS

L_{S1}	77.22 μH
L_{S2}	1.55 μH
M_{PS1}	14.96 μH
M_{PS2}	1.38 μH
M_{12}	6.49 μH
R_{S1}	0.33 Ω
R_{S2}	0.04 Ω
C_{S1}	28.63 nF
C_{S1P}	27.27 nF
C_{S2}	924.5 nF
C_{LP}	51.30 nF

is also applicable to other resonant WPT system. An example of implementing the proposed idea in a series-parallel resonant WPT system is given in the Appendix.

VI. EXPERIMENTAL VERIFICATION

Experiments are carried out based on the 10 W WPT system using the coils shown in Fig. 5 and the topology shown in Fig. 12(a). The receiver coil is split into two coils with ten turns and one turn, respectively, as shown in Fig. 21. As mode switching will only be activated after the power supply is shut down, the switches could be easily controlled with microprocessors monitoring the load resistance range. In experiments, mode switching is done manually to measure the efficiency of the system. Table II shows the parameters of the proposed structure and circuit. Since the lead wires, which are

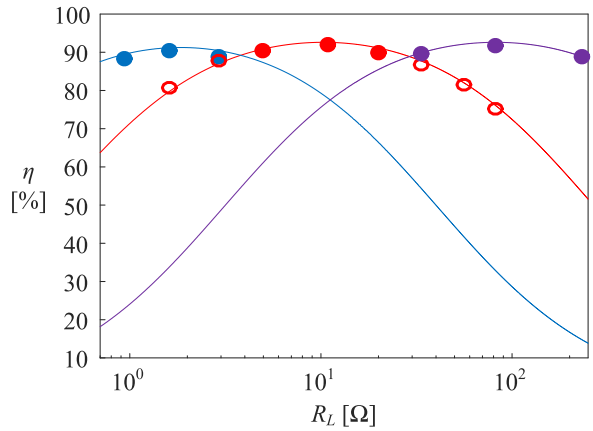

Fig. 22. Measured efficiency of the proposed universal system (solid dots); measured efficiency of the two-coil system with load resistance not in the high-efficiency range (hollow dots); and the theoretical efficiency curves of 3 operation modes (real lines; blue: three-coil mode; red: two-coil mode; purple: two-coil with parallel capacitor mode).

used to connect the coil and the compensation circuit, are not considered in the theoretical analysis, the self-inductance of the one-turn coil is a little larger than the value used in the analysis, i.e., L_{S2} is 1.55 μH (theoretical value 1.13 μH). Therefore, an optimization is carried out based on the practical inductances and the optimal capacitances are all listed in Table II. Fig. 22 shows three sets of practical energy efficiency measurements and their corresponding theoretical efficiency curves under the

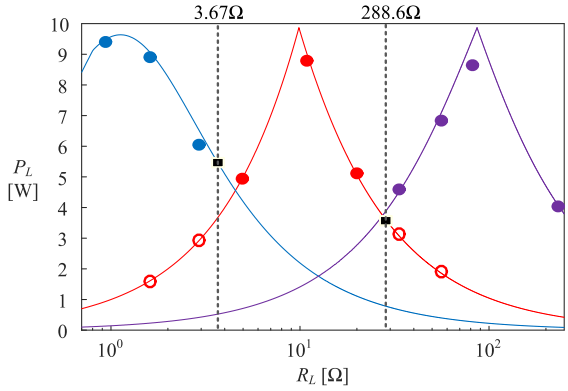

Fig. 23. Measured output power of the proposed universal system with 1 A limitation in the coil current (solid dots); measured output power of the two-coil system with load resistance not in the high-efficiency range (hollow dots); and the theoretical output power curves of three operation modes (real lines; blue: three-coil mode; red: two-coil mode; purple: two-coil with parallel capacitor mode).

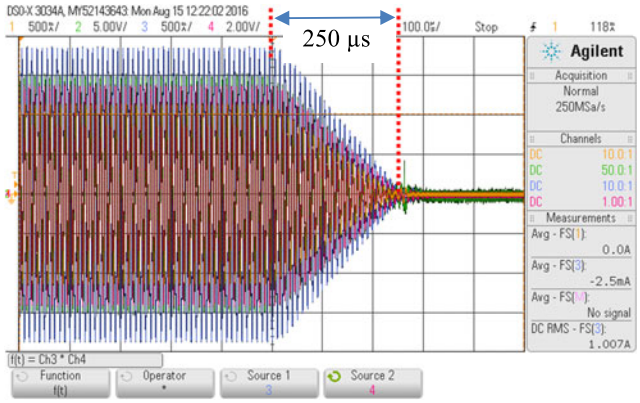

Fig. 24. Input voltage, primary current, secondary current, and output voltage of the universal WPT system operating in three-coil mode with a load resistance of 2.93 Ω (time scale: 100 μs/div).

three operating modes. These measurements agree well with the calculations. These practical measurements confirm the proposed idea that the reconfigurable WPT circuit can achieve high energy efficiency over a very wide load resistance range. Fig. 23 shows the output power of the proposed system with a limitation of 1 A in the coil current. Again, the measurements totally verify the theoretical analysis.

Fig. 24 shows that after the power supply is shut down, the voltages and currents in the system will fade away in about 250 μs. Therefore, the mode switching can be conducted after this very short delay time and therefore the overall charging time will not be affected.

VII. Conclusion

By splitting the receiver winding, the optimum load resistance (at which high efficiency can be achieved) can be extended to the low load resistance range. With the use of parallel capacitor across the load, the optimum load resistance can be extended to the high load resistance range. Taking advantages of these two complementary approaches, this study shows that using reconfigurable WPT systems can achieve high energy efficiency

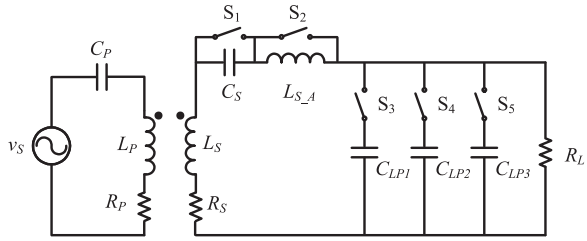

Fig. 25. Possible configuration of an SP compensated for enlarging high-efficiency load range.

operation over a very wide load range and simultaneously keeping the volt–amp ratings of the coils low. Theoretical analysis of this new concept has been presented with explanations. This new theoretical concept has been confirmed with practical measurements. The proposal offers a new approach to achieve high energy efficiency in medium- and high-power applications in which energy efficiency is of paramount importance.

Appendix
Possible Reconfigurable Topology for SP Compensated WPT

There will be three operation modes. In Fig. 25, $C_{LP1} > C_{LP2} > C_{LP3}$:

1) For $R_{\min} < R_L < R_1$: S_2, S_3 on; S_1, S_4, S_5 off. The resonant tank is formed by L_S, C_S and C_{LP1}.
2) For $R_1 < R_L < R_2$: S_1, S_2, S_4 on; S_3, S_5 off. The resonant tank is formed by L_S and C_{LP2}.
3) For $R_2 < R_L < R_{\max}$: S_1, S_5 on; S_2, S_3, S_4 off. The resonant tank is formed by L_S, L_{S_A}, and C_{LP3}.

The second operation mode is the normal SP compensation in which L_S and C_{LP2} are resonant at the operating frequency. Proper values of the components should be chosen for different given load range.

References

[1] G. A. Covic and J. T. Boys, "Inductive power transfer," *Proc. IEEE*, vol. 101, no. 6, pp. 1276–1289, Jun. 2013.
[2] S. Y. R. Hui, "Planar wireless charging technology for portable electronic products and qi," *Proc. IEEE*, vol. 101, no. 6, pp. 1290–1301, Jun. 2013.
[3] Sep. 2017. [Online]. Available: http://www.wirelesspowerconsortium.com
[4] M. Budhia, G. A. Covic, and J. T. Boys, "Design and optimization of circular magnetic structures for lumped inductive power transfer systems," *IEEE Trans. Power Electron.*, vol. 26, no. 11, pp. 3096–3108, Nov. 2011.
[5] C. Mi, G. Buja, S. Y. Choi, and C. T. Rim, "Modern advances in wireless power transfer systems for roadway powered electric vehicles," *IEEE Trans. Ind. Electron.*, vol. 63, no. 10, pp. 6533–6545, Oct. 2016.
[6] S. Ahn, N. P. Suh, and D. H. Cho, "Charging up the road," *IEEE Spectr.*, vol. 50, no. 4, pp. 48–54, Mar. 2013.
[7] J. S. Ho, S. Kim, and A. S. Y. Poon, "Midfield wireless powering for implantable systems," *Proc. IEEE*, vol. 101, no. 6, pp. 1369–1378, Jun. 2013.
[8] H. M. Lee, M. Kiani, and M. Ghovanloo, "Advanced wireless power and data transmission techniques for implantable medical devices," in *Proc. IEEE Custom Integrated Circuits Conf.*, Sep. 2015, pp. 1–8.
[9] P. Si, A. P. Hu, S. Malpas, and D. Budgett, "A frequency control method for regulating wireless power to implantable devices," *IEEE Trans. Biomed. Circuits Syst.*, vol. 2, no. 1, pp. 22–29, Mar. 2008.

[10] M. Fu, C. Ma, and X. Zhu, "A cascaded boost–buck converter for high-efficiency wireless power transfer systems," *IEEE Trans. Ind. Inf.*, vol. 10, no. 3, pp. 1972–1980, Aug. 2014.
[11] M. Fu, H. Yin, X. Zhu, and C. Ma, "Analysis and tracking of optimal load in wireless power transfer systems," *IEEE Trans. Power Electron.*, vol. 30, no. 7, pp. 3952–3963, Jul. 2015.
[12] W. X. Zhong and S. Y. R. Hui, "Maximum energy efficiency tracking for wireless power transfer systems," *IEEE Trans. Power Electron.*, vol. 30, no. 7, pp. 4025–4034, Jul. 2015.
[13] D. Ahn, S. Kim, J. Moon, and I. K. Cho, "Wireless power transfer with automatic feedback control of load resistance transformation," *IEEE Trans. Power Electron.*, vol. 31, no. 11, pp. 7876–7886, Nov. 2016.
[14] H. Li, J. Li, K. Wang, W. Chen, and X. Yang, "A maximum efficiency point tracking control scheme for wireless power transfer systems using magnetic resonant coupling," *IEEE Trans. Power Electron.*, vol. 30, no. 7, pp. 3998–4008, Jul. 2015.
[15] L. Yuan, B. Li, Y. Zhang, F. He, K. Chen, and Z. Zhao, "Maximum efficiency point tracking of the wireless power transfer system for the battery charging in electric vehicles," in *Proc. 18th Int. Conf. Electr. Mach. Syst.*, Pattaya, 2015, pp. 1101–1107.
[16] D. Ahn and S. Hong, "Wireless power transfer resonance coupling amplification by load-modulation switching controller," *IEEE Trans. Ind. Electron.*, vol. 62, no. 2, pp. 898–909, Feb. 2015.
[17] M. Kiani, B. Lee, P. Yeon, and M. Ghovanloo, "A Q-modulation technique for efficient inductive power transmission," *IEEE J. Solid-State Circuits*, vol. 50, no. 12, pp. 2839–2848, Dec. 2015.
[18] D. Kobayashi, T. Imura, and Y. Hori, "Real-time coupling coefficient estimation and maximum efficiency control on dynamic wireless power transfer using secondary DC–DC converter," in *Proc. 41st Annu. Conf. IEEE Ind. Electron. Soc.*, Yokohama, 2015, pp. 004650–004655.
[19] R. Mai, Y. Liu, Y. Li, P. Yue, G. Cao, and Z. He, "An active rectifier based maximum efficiency tracking method using an additional measurement coil for wireless power transfer," *IEEE Trans. Power Electron.*, (early access).
[20] W. Zhong and S. Y. R. Hui, "Charging time control of wireless power transfer systems without using mutual coupling information and wireless communication system," *IEEE Trans. Ind. Electron.*, vol. 64, no. 1, pp. 228–235, Jan. 2017.
[21] T. C. Beh, T. Imura, M. Kato, and Y. Hori, "Basic study of improving efficiency of wireless power transfer via magnetic resonance coupling based on impedance matching," *in Proc. IEEE Int. Symp. Ind. Electron.*, Bari, 2010, pp. 2011–2016.
[22] K. Silay *et al.*, "Load optimization of an inductive power link for remote powering of biomedical implants," in *Proc. IEEE Int. Symp. Circuits Syst.*, 2005, pp. 533–536.
[23] R. Xue, K. Cheng, and M. Je, "High-efficiency wireless power transfer for biomedical implants by optimal resonant load transformation," *IEEE Trans. Biomed. Circuits Syst.*, vol. 60, no. 4, pp. 867–874, Apr. 2013.
[24] A. Kurs, A. Karalis, R. Moffatt, J. D. Joannopoulos, P. Fisher, and M. Soljacic, "Wireless power transfer via strongly coupled magnetic resonances," *Sci. Express*, vol. 317, pp. 83–86, Jul. 2007.
[25] A. P. Sample, D. A. Meyer, and J. R. Smith, "Analysis, experimental results, and range adaptation of magnetically coupled resonators for wireless power transfer," *IEEE Trans. Ind. Electron.*, vol. 58, no. 2, pp. 544–554, Feb. 2011.
[26] M. Kiani, U. Jow, and M. Ghovanloo, "Design and optimization of a 3-coil inductive link for efficient wireless power transmission," *IEEE Trans. Biomed. Circuits Syst.*, vol. 5, no. 6, pp. 579–591, Dec. 2011.
[27] W. X. Zhong, C. Zhang, X. Liu, and S. Y. R. Hui, "A methodology for making a 3-coil wireless power transfer system more energy efficient than a 2-coil counterpart for extended transmission distance," *IEEE Trans. Power Electron.*, vol. 30, no. 2, pp. 933–942, Feb. 2015.
[28] Y. K. Jung and B. Lee, "Design of adaptive optimal load circuit for maximum wireless power transfer efficiency," in *Proc. Asia-Pacific Microwave Conf.,* Seoul, 2013, pp. 1221–1223.
[29] Y. Lim, H. Tang, S. Lim, and J. Park, "An adaptive impedance-matching network based on a novel capacitor matrix for wireless power transfer," *IEEE Trans. Power Electron.*, vol. 29, no. 8, pp. 4403–4413, Aug. 2014.
[30] G. Lee, B. H. Waters, Y. G. Shin, J. R. Smith, and W. S. Park, "A reconfigurable resonant coil for range adaptation wireless power transfer," *IEEE Trans. Microw. Theory Tech.*, vol. 64, no. 2, pp. 624–632, Feb. 2016.
[31] T. C. Beh, M. Kato, T. Imura, S. Oh, and Y. Hori, "Automated impedance matching system for robust wireless power transfer via magnetic resonance coupling," *IEEE Trans. Ind. Electron.*, vol. 60, no. 9, pp. 3689–3698, Sep. 2013.
[32] Q. Chen, S. Wong, C. Tse, and X. Ruan, "Analysis, design, and control of a transcutaneous power regulator for artificial hearts," *IEEE Trans. Biomed. Circuits Syst.*, vol. 3, no. 1, pp. 23–31, Feb. 2009.
[33] D. Ahn and S. Hong, "Wireless power transmission with self-regulated output voltage for biomedical implant," *IEEE Trans. Ind. Electron.*, vol. 61, no. 5, pp. 2225–2235, May 2014.
[34] D. Patil, M. Sirico, L. Gu, and B. Fahimi, "Maximum efficiency tracking in wireless power transfer for battery charger: Phase shift and frequency control," in *Proc. IEEE Energy Convers. Congr. Expo.*, Milwaukee, WI, USA, 2016, pp. 1–8.

Wenxing Zhong (M'13) received the B.Eng. degree in electrical engineering from Tsinghua University, Beijing, China, in 2007, and the Ph.D. degree from the City University of Hong Kong, Kowloon, Hong Kong, in 2012.

He is currently a Professor in the Department of Electrical Engineering, Zhejiang University, China. From March 2016 to May 2017, he was a Research Assistant Professor in the Department of Electrical and Electronic Engineering, The University of Hong Kong, Pokfulam, Hong Kong. His current research interests include wireless power transfer and power electronics.

Dr. Zhong has received two Transaction First Prize Paper Awards from the IEEE Power Electronics Society since 2015.

S. Y. (Ron) Hui (M'87–SM'94–F'03) received the B.Sc. (Eng. Hons.) degree in electrical and electronic engineering from the University of Birmingham, Birmingham, U.K., in 1984, and the D.I.C. and Ph.D. degrees in electrical engineering from the Imperial College London, London, U.K., in 1987.

He currently holds the Philip Wong Wilson Wong Chair Professorship at the University of Hong Kong, Pokfulam, Hong Kong, and a part-time Chair Professorship at the Imperial College London. He has authored or coauthored over 300 technical papers, including more than 230 refereed journal publications. Over 60 of his patents have been adopted by industry. His inventions on wireless charging platform technology underpin key dimensions of Qi, the world's first wireless power standard, with freedom of positioning and localized charging features for wireless charging of consumer electronics. He developed the photo-electro-thermal theory for LED systems.

Dr. Hui is an Associate Editor of the IEEE TRANSACTIONS ON POWER ELECTRONICS and the IEEE TRANSACTIONS ON INDUSTRIAL ELECTRONICS, and an Editor of the IEEE JOURNAL OF EMERGING AND SELECTED TOPICS IN POWER ELECTRONICS. He received the IEEE Rudolf Chope R&D Award from the IEEE Industrial Electronics Society and the IET Achievement Medal (The Crompton Medal) in 2010, and IEEE William E. Newell Power Electronics Award in 2015. He is a Fellow of the Australian Academy of Technology and Engineering and also a Fellow the Royal Academy of Engineering, U.K.